ELECTRONIC SUPPLEMENTARY MATERIAL

Surface-Confined Fluorescence Enhancement of Au Nanoclusters Anchoring to A Two-Dimensional Ultrathin Nanosheet toward Bioimaging

Rui Tian, Dongpeng Yan, Chunyang Li, Simin Xu, Ruizheng Liang,* Lingyan Guo,

Min Wei,* David G. Evans, and Xue Duan

State Key Laboratory of Chemical Resource Engineering, Beijing University of Chemical Technology, Beijing 100029, P. R. China

* Corresponding authors. Tel: +86-10-64412131; Fax: +86-10-64425385.

E-mail addresses: liangruizheng2000@163.com (R. Liang); weimin@mail.buct.edu.cn (M. Wei).

1. Experimental Section

Materials

L-Glutathione in the reduced form (GSH) was obtained from Sigma−Aldrich. Hydrogen tetrachloroaurate hydrate ($HAuCl_4•3H_2O$, >99.9%), analytical-grade chemicals including formamide, $Mg(NO_3)_2•6H_2O$, $Al(NO_3)_3•9H_2O$ and HNO_3 were purchased from Aladdin Chemical. Co. Ltd. Ultrapure water from a Milli-Q Millipore system was used as the general solvent in all the experimental processes.

Preparation of Au NCs and Au NCs/ELDH Hybrid Material

The aqueous synthesis of GSH reduced Au NCs was similar to the reported method,[1] but with some modifications. In a typical synthesis, $HAuCl_4•3H_2O$ (20 mM, 6.0 mL) was mixed with GSH (100 mM, 1.80 mL), followed by adding 52 mL of ultrapure water at room temperature. The above solution (60 mL) was transferred to a stainless-steel Teflon-lined autoclave. After reaction at 70 °C for 24 h, the autoclave was cooled down naturally to room temperature. The obtained Au NCs was purified by the dialysis membrane for 24 h and finally stored at 4 °C for use. The preparation of MgAl-LDH nanosheets was similar with our previous work.[2] Formamide (100 mL) was used to exfoliate the as-prepared nitrate MgAl-LDH (0.1 g) microcrystals to obtain a colloidal suspension of MgAl-LDH nanosheets (denoted as ELDH). Powerful ultrasonic was used to break the nanosheets to ~100 nm. Au NCs sol (2 mM) was dropwisely added into the ELDH suspension (1g/L) with various Au NCs/ELDH ratios under continuous shaking, and the resulting suspension was shaken for another 10 min at room temperature. After a centrifugation at 10000 r/min for 20 min, the Au NCs/ELDH hybrid material was withdrawn and re-dispersed in water for further use.

Reference samples were prepared by immobilizing Au NCs onto other substrates, respectively, including montmorillonoid (MMT, electronegative), graphene oxide (GO, electronegative), poly-diallyldimethylammonium chloride (PDDA, electropositive) and ELDH with different metallic composition (CoAl-ELDH and CoNi-ELDH, electropositive), are fabricated in the similar way with the ratio of Au NCs/substrate at 3:1.

Bio-imaging Studies on Hela Cells

Hela cells were grown and expanded in 25 cm^2 cell-culture flask. After reaching 80–90% confluence, the Hela cells were washed with PBS, afterwards detached from the flask by addition of 1.0 mL of 0.25% trypsin for 5 min at 37 °C. Hela cells were seeded into plates with 100 μL of medium at a density of 1×10^4 cells/well for 24 h, followed by treating with pristine Au NCs, LDH and Au NCs_3/$ELDH_1$ with different concentrations for 24 h. The colorimetric 3-(4,5-dimethylthiazol-2-yl)-2,5-diphenyltetrazolium bromide (MTT) was used to determine the cell viability. In a typical cellular imaging experiment, the cells were seeded into 96-well plate and incubated with different concentrations (6.25–100 μg/mL) of Au NCs and Au NCs_3/$ELDH_1$ for 24 h. After washing with PBS for three times, a confocal microscopy was used to evaluate the imaging effect through capturing their fluorescence images with the two-photon excitation wavelength at 720 nm. Stability in cell culture has been investigated for continuous capture for 10 min excited by 720 nm.

Sample Characterizations

Transmission electron microscope (TEM) images were recorded on a JEOL JEM-2100 TEM with the accelerating voltage of 200 kV. The UV-vis absorption spectra were collected in the range from 300 to 600 nm on a Shimadzu U-3000 spectrophotometer, with the slit width of 1.0 nm. The fluorescence spectra were performed on a RF-5301PC fluorospectrophotometer with

the excitation wavelength of 360 nm. The fluorescence emission spectra range in 400–700 nm, and the width of both the excitation and emission slit is 5 nm. X-ray photoelectron spectroscopy (XPS) measurements were performed using an ESCALAB 250 instrument (Thermo Electron) with Al Ka radiation. Steady–state luminescence lifetime measurements were recorded with an Edinburgh FLS 980 lifetime and steady state spectrometer. The elemental content of samples was determined by inductively coupled plasma (ICP) emission spectroscopy on a Shimadzu ICPS-7500 instrument. The particle size distribution and zeta potential analysis were carried out using a Malvern Mastersizer 2000 laser particle size analyzer. The cell imaging was performed on a TCS SP5 two-photon confocal microscope (Leica). Electrochemical impedance spectroscopy (EIS) tests were performed by applying an AC voltage with 5 mV amplitude in a frequency range from 100 kHz to 0.1 Hz.

2. Computational Details

Model Construction: The model of Au NC is constructed in the same way as our previous work,[3] and the model contains 36 Au atoms and 12 peptides. The models of MgAl-LDH, CoAl-LDH and CoNi-LDH are constructed according to their powder X-ray diffraction data. The space group of these three LDHs is $r\bar{3}m$, with unit cell parameters: $\alpha = \beta = 90°$, $\gamma = 120°$. The LDHs supercell is constructed as 3 × 3 × 1 in the *a*-, *b*- and *c*-direction since the molar ratio of M^{2+}/M^{3+} is 2, and 9 nitrate anions are introduced into the interlayer gallery of MgAl-LDH, CoAl-LDH and CoNi-LDH.

The models of Au NCs/MgAl-ELDH, Au NCs/CoAl-ELDH and Au NCs/CoNi-ELDH are constructed in a similar way as the above mentioned LDH models. The supercell of Au NCs/ELDH is 6 × 4 × 1 in the *a*-, *b*- and *c*-direction, and two Au NCs are localized on ELDH in each model (Au NCs/MgAl-ELDH, Au NCs/CoAl-ELDH and Au NCs/CoNi-ELDH).

Computational Method: The density functional theory plus Hubbard correction (DFT+U) calculations are performed on MgAl-LDH, CoAl-LDH, CoNi-LDH and Au NCs with the CASTEP code in the Materials Studio,[4] version 6.1 software package (Accelrys software Inc., San Diego, CA). The DFT calculations are carried out with a plane wave implementation at the generalized gradient approximation (GGA) Perdew-Burke-Ernzerhof (PBE) level.[5] Hubbard correction is applied to correct the well-known DFT self-interaction errors for the strongly correlated electrons in the first-row transition metal (Co and Ni here). In this work, the value of $U - J$ (U_{eff}) is 3.52 eV for Co[6] and 3.8 eV for Ni[7], respectively. The structure optimization is based on the following criteria: (1) an energy tolerance of 1×10^{-5} eV per atom, (2) a maximum force tolerance of 0.03 eV/Å, and (3) a maximum displacement tolerance of 1×10^{-3} Å. The work function is the minimum thermodynamic energy needed to remove an electron in the Fermi level of the LDH to a point in the vacuum immediately outside the LDH surface, which is calculated with eq. 1:

$$W = -e\phi - E_{\text{F}} \quad (1)$$

where e is the charge of an electron; ϕ is the electrostatic potential in the vacuum nearby the LDH surface, and E_{F} is the Fermi level inside the LDH. Then, the energy difference (x) between the Fermi level (E_{F}) and CBM (E_{CBM}) can be obtained from the band structures of MgAl-LDH, CoAl-LDH and CoNi-LDH, respectively, as shown in eq. 2:

$$x = E_{\text{CBM}} - E_{\text{F}} \quad (2)$$

Subsequently, the band edge placement of these three LDHs can be deduced by eq. 3 and eq. 4:

$$E_{CBM} = E_F + x = -W + x \quad (3)$$

$$E_{VBM} = E_{CBM} - E_g = -W + x - E_g \quad (4)$$

where E_{g} is the band gap of LDH.

Molecular dynamics simulations are performed on model Au NCs/MgAl-ELDH, Au NCs/CoAl-ELDH and Au NCs/CoNi-ELDH in isothermal-isobaric (*NPT*) ensemble with the temperature of 298 K and the pressure of 0.1 MPa. The Universal force field is adopted. Temperature and pressure control are performed using the Andersen method[8] and the Berendsen method,[9] respectively. The long-range coulombic interactions are computed by the Ewald summation technique.[10] The time step is set to be 1 fs and the simulation time is 5 ns.

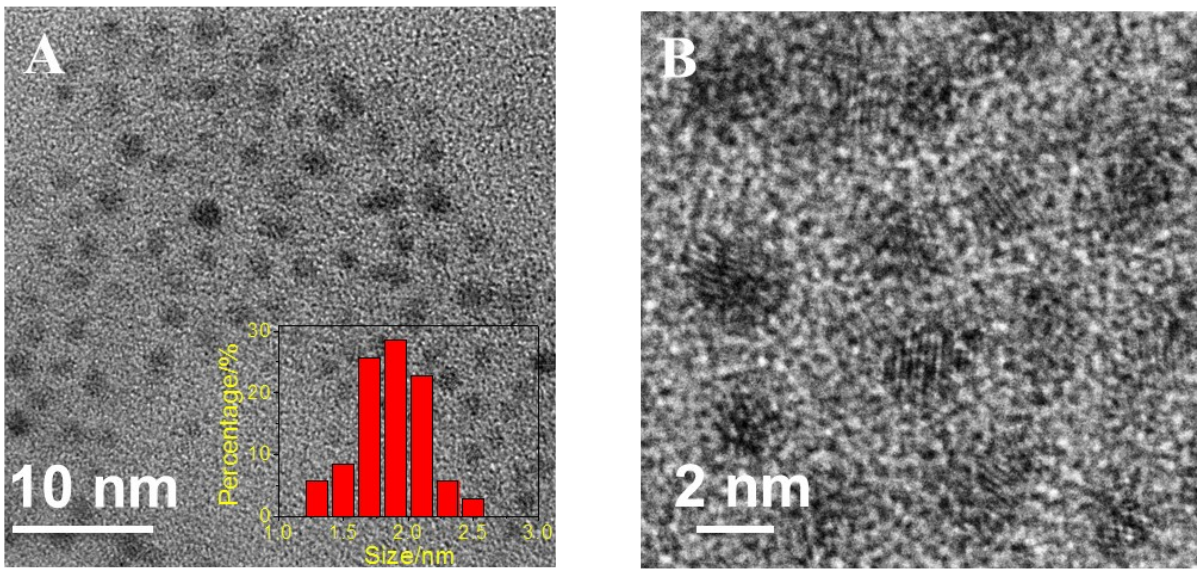

Fig. S1 High resolution TEM images of Au NCs: (A) low magnification (the inset shows the size distribution) and (B) high magnification (with crystal lattice).

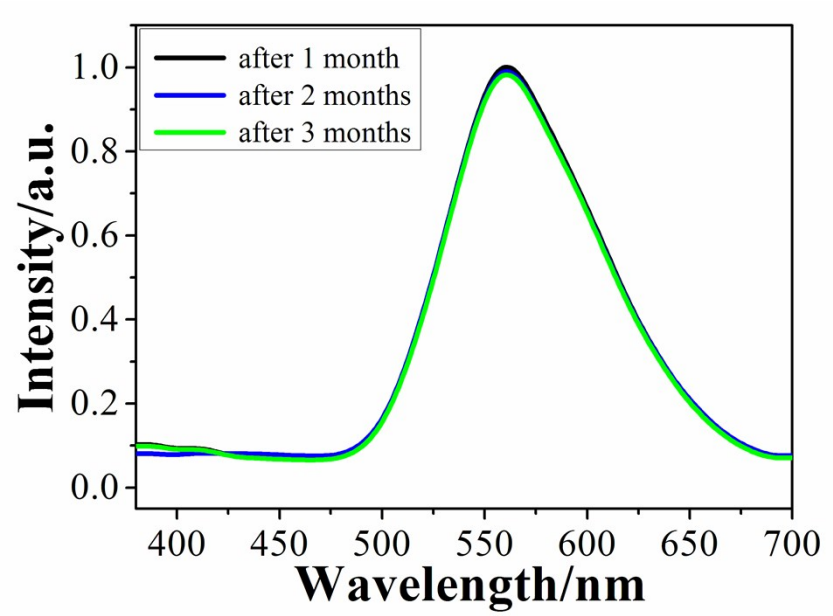

Fig. S2 Fluorescence spectra of Au NCs_3/$ELDH_1$ nanohybrid recorded within three months.

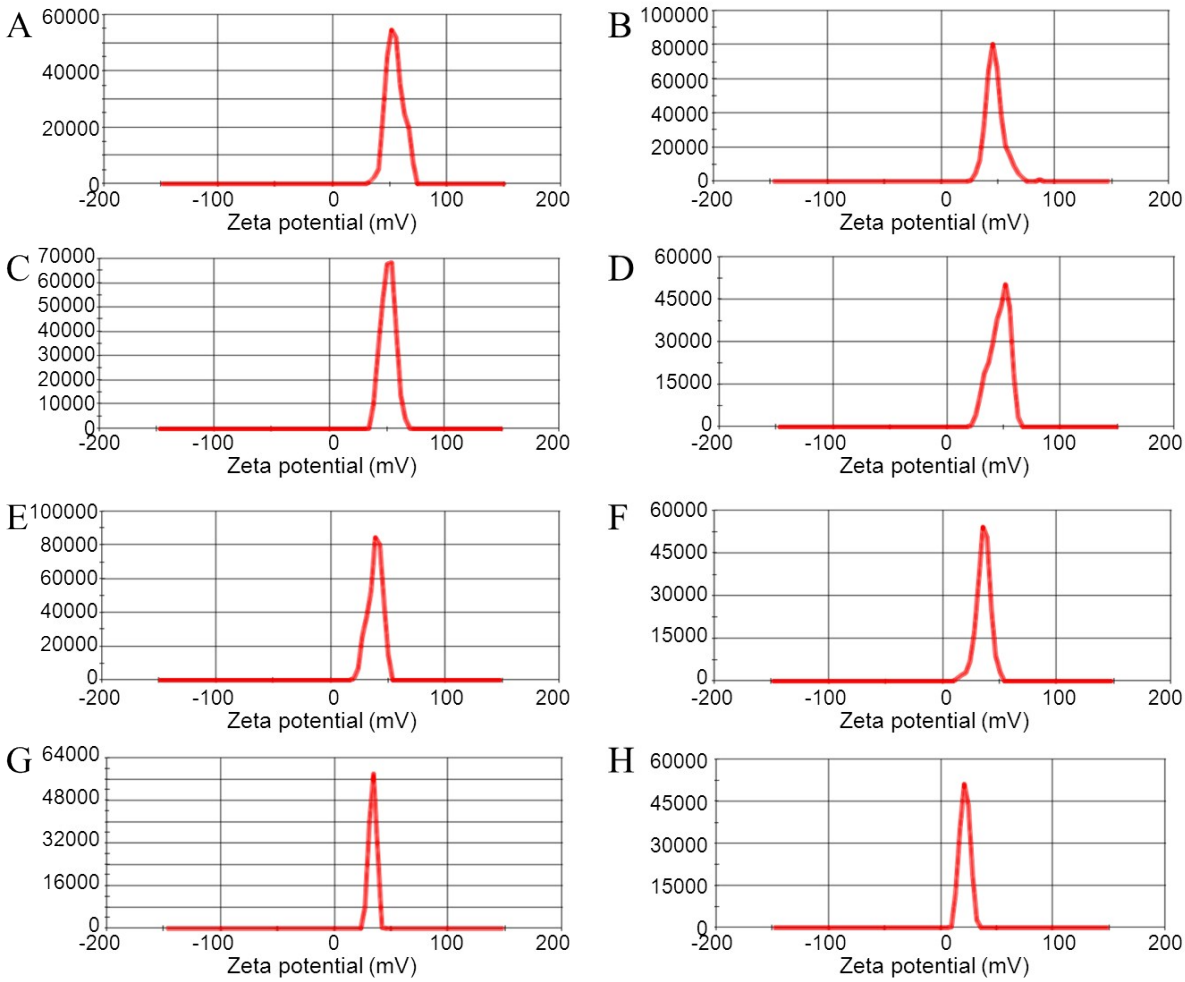

Fig. S3 Zeta potential of Au NCs_x/$ELDH_y$ with various ratios (from A to H, x/y=0:1, 0.5:1, 0.75:1, 1:1, 1.25:1, 1.5:1, 2:1, and 4:1, respectively).

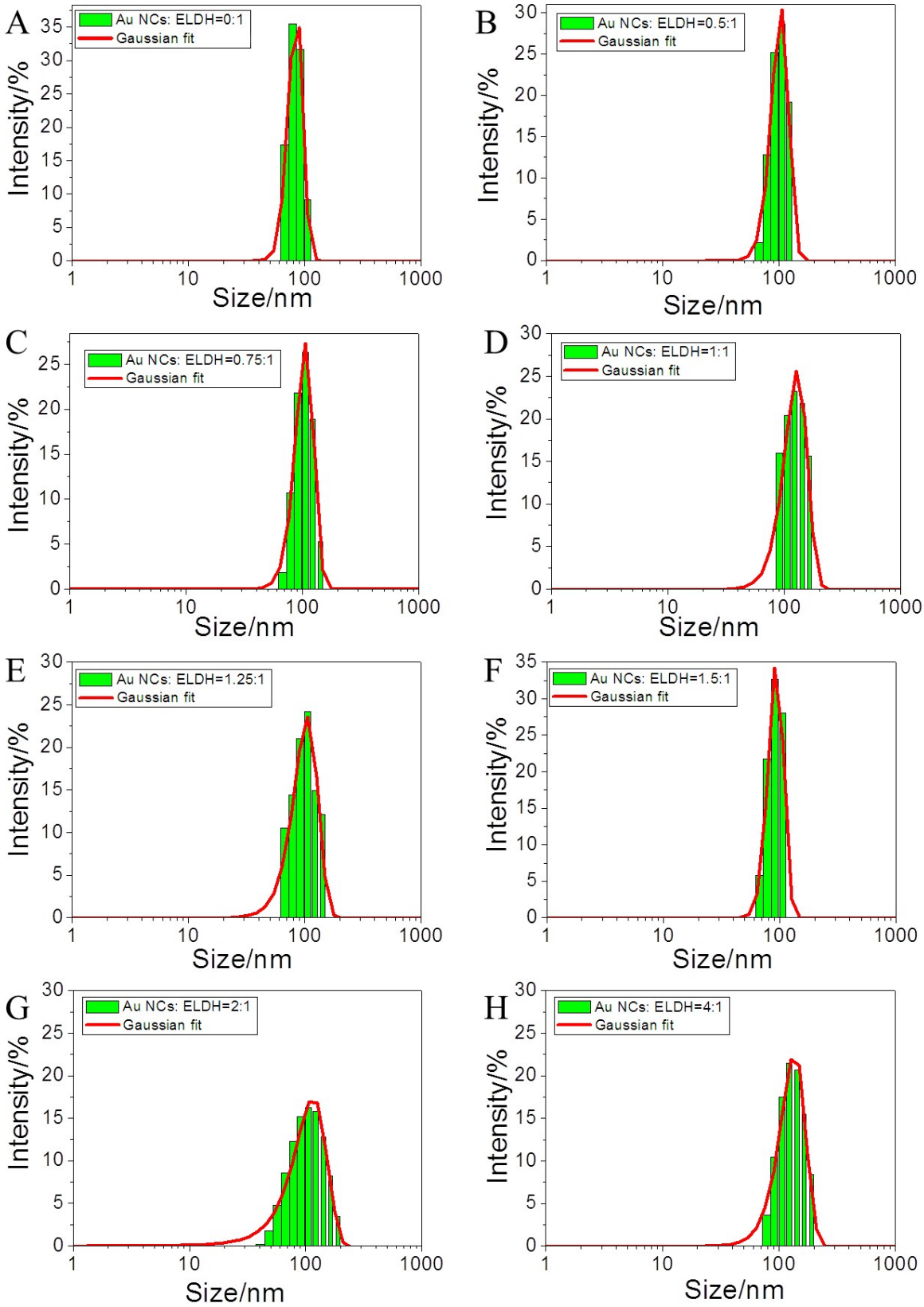

Fig. S4 Size distribution of Au NCs_x/$ELDH_y$ with various ratios (from A to H, *x*/*y*=0:1, 0.5:1, 0.75:1, 1:1, 1.25:1, 1.5:1, 2:1, and 4:1, respectively).

Table S1. Zeta potential and size distribution of Au NCs_x/$ELDH_y$ hybrid materials

No.	Sample	Size/nm	Zeta potential/mV
10	Au NCs aqueous	2.310	–7.21
1	Au NCs: ELDH=0:1	83.65	54.4
2	Au NCs: ELDH=0.5:1	102.5	47.1
3	Au NCs: ELDH=0.75:1	103.8	49.4
4	Au NCs: ELDH=1:1	142.1	46.2
5	Au NCs: ELDH=1.25:1	106.8	45.0
6	Au NCs: ELDH=1.5:1	94.96	36.2
7	Au NCs: ELDH=2:1	108.8	38.8
8	Au NCs: ELDH=3:1	112.3	33.8
9	Au NCs: ELDH=4:1	133.3	30.7

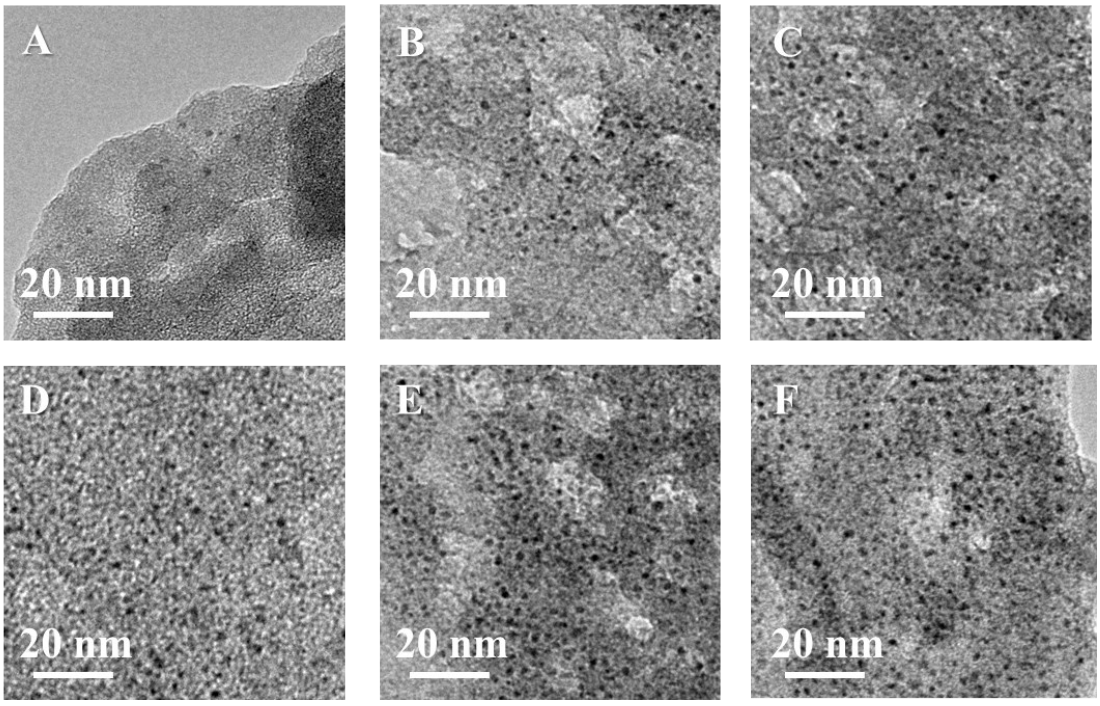

Fig. S5 TEM images of Au NCs_x/$ELDH_y$ hybrid materials prepared with various ratios (from A to F, x/y= 0.5:1, 0.75:1, 1:1, 1.5:1, 2:1, and 4:1, respectively).

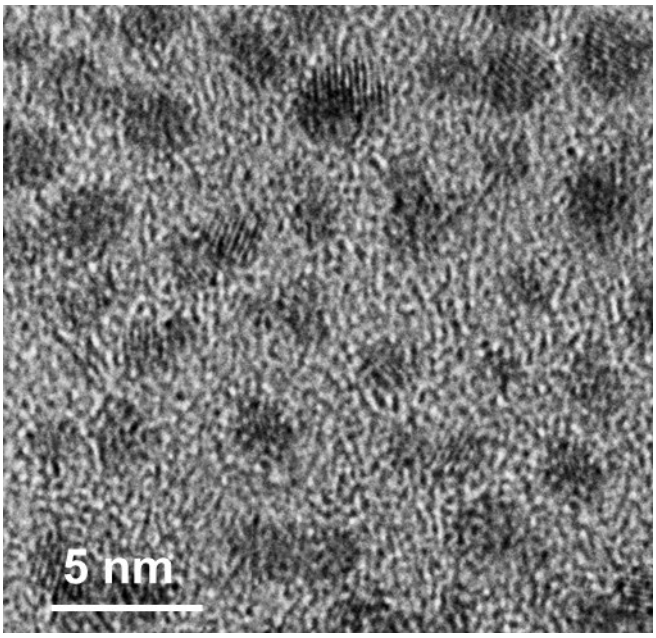

Fig. S6 HRTEM image of Au $NCs_3/ELDH_1$ nanohybrid.

Table S2. Loading density of Au for Au $NCs_x/ELDH_y$ samples with various *x/y* ratios

Sample	Nominal molar ratio of Au:ELDH	Determined molar ratio of Au:ELDH
Au $NCs_{0.5}/ELDH_1$	0.28	0.42
Au $NCs_{0.75}/ELDH_1$	0.42	0.57
Au $NCs_1/ELDH_1$	0.56	0.87
Au $NCs_{1.25}/ELDH_1$	0.69	1.02
Au $NCs_{1.5}/ELDH_1$	0.83	1.29
Au $NCs_2/ELDH_1$	1.11	2.09
Au $NCs_3/ELDH_1$	1.67	3.17
Au $NCs_4/ELDH_1$	2.22	2.90

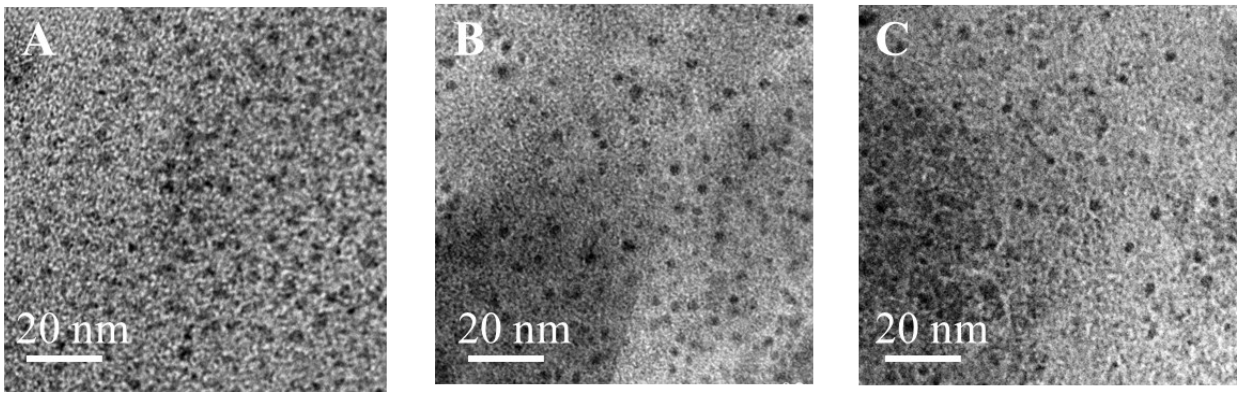

Fig. S7 TEM images of Au NCs_3/$ELDH_1$ hybrid material prepared by MgAl-LDH nanosheets with different molar ratios of Mg/Al: (A) 2:1, (B) 3:1 and (C) 4:1.

Table S3. Quantum yields (QY) of Au NCs_x/$ELDH_y$ with various *x*/*y* ratios

No.	Sample	Abs.	PL Intensity	QY
10	Au NCs aqueous	0.0624	7031.5	2.60
1	Au NCs: ELDH=0:1	0.0355	242.2	0.16
2	Au NCs: ELDH=0.5:1	0.0879	9978.5	2.71
3	Au NCs: ELDH=0.75:1	0.0759	10678.1	3.22
4	Au NCs: ELDH=1:1	0.0964	19435.4	4.61
5	Au NCs: ELDH=1.25:1	0.0968	22953.9	5.42
6	Au NCs: ELDH=1.5:1	0.0689	29216.6	9.70
7	Au NCs: ELDH=2:1	0.0712	44279.8	14.23
8	Au NCs: ELDH=3:1	0.0556	46321.5	19.05
9	Au NCs: ELDH=4:1	0.0571	36757.2	14.73

The fluorescence QY of luminescence materials was determined relative to rhodamine-6G (QY=0.95) using the relation:

$$QY_x = \frac{A_s n_x^2 F_x}{A_x n_s^2 F_s} QY_s \quad (5)$$

where F_x and F_s are the total integrated fluorescence intensity of the unknown and emission standard, respectively; A_x and A_s are the corresponding wavelength-specific absorbance, and QY_s is the fluorescence QY value for the standard fluorophore. The value of $(n_x/n_s)^2$ represents the solvent refractive index correction.[11]

Table S4. QYs of Au NCs_3/MgAl-$ELDH_1$ with various molar ratios of Mg/Al in ELDH

Mg:Al	Abs.	PL Intensity	QY
2:1	0.0556	46321.5	19.05
3:1	0.0612	46519.2	17.40
4:1	0.0880	55121.5	14.33

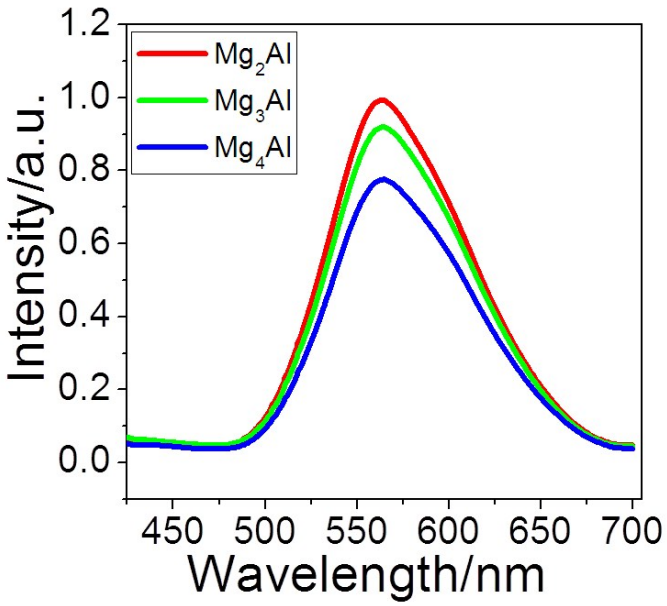

Fig. S8 Fluorescence emission spectra of Au NCs_3/MgAl-$ELDH_1$ hybrid material (equivalent Au) with various molar ratios of Mg/Al in ELDH: 2:1, 3:1 and 4:1, respectively.

Table S5. The fitting of fluorescence decay data of pristine Au NCs and Au $NCs_x/ELDH_y$

Samples	τ_i (μs)[a]	A_i (%)	<τ> (μs)	χ^{2}[b]
Pristine Au NCs	0.538	44.10	1.998	1.570
	3.151	55.92		
Au $NCs_{0.5}/ELDH_1$	5.425	24.63	12.77	1.467
	15.17	75.37		
Au $NCs_{0.75}/ELDH_1$	5.691	23.31	13.03	1.379
	15.26	76.69		
Au $NCs_1/ELDH_1$	5.947	22.49	13.05	1.328
	15.11	77.51		
Au $NCs_{1.25}/ELDH_1$	6.055	24.47	12.87	1.656
	18.08	75.53		
Au $NCs_{1.5}/ELDH_1$	6.138	21.99	13.05	1.522
	15.00	78.01		
Au $NCs_2/ELDH_1$	5.969	23.91	13.25	1.517
	15.54	76.09		
Au $NCs_3/ELDH_1$	6.247	20.61	13.99	1.306
	16.01	79.39		
Au $NCs_4/ELDH_1$	5.896	23.07	12.88	1.464
	14.98	76.93		

[a] τ_i (i =1, 2) is the fitted fluorescence lifetime. A_i is the percentage of τ_i. In this case, <τ> = $\Sigma A_i\tau_i$; ΣA_i=1). [b] The goodness of fit is indicated by the value of χ^2.

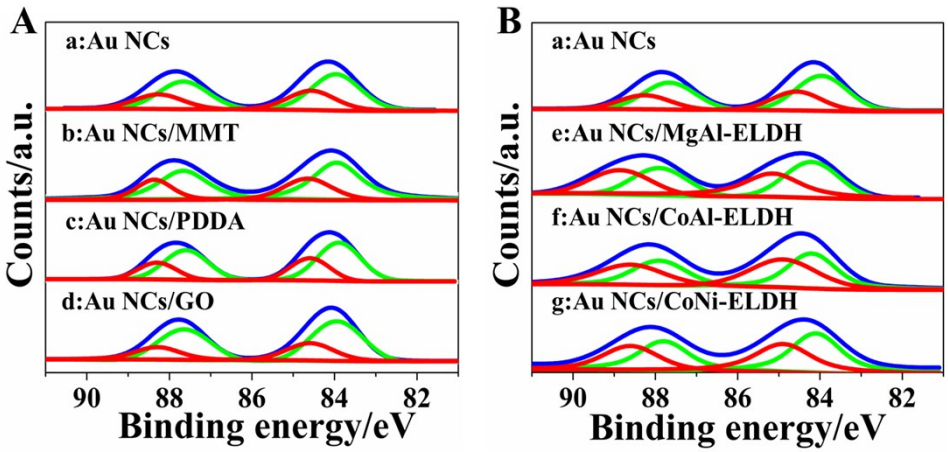

Fig. S9 (A, B) XPS analysis of (a) pristine Au NCs, (b) Au NCs/MMT, (c) Au NCs/PDDA, (d) Au NCs/GO, (e) Au NCs/MgAl-ELDH, (f) Au NCs/CoAl-ELDH and (g) Au NCs/CoNi-ELDH, respectively. Blue line: total Au species; green line: Au(0); red line: Au(I).

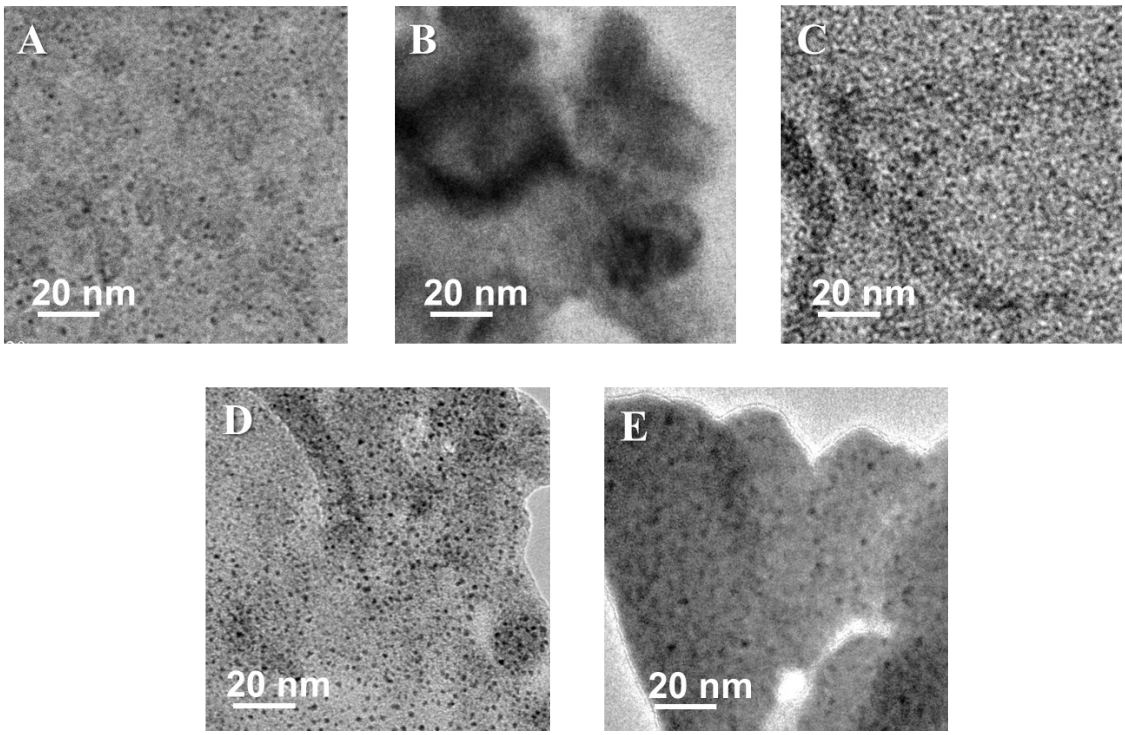

Fig. S10 TEM images of (A) Au NCs/MMT, (B) Au NCs/PDDA, (C) Au NCs/GO, (D) Au NCs/CoAl-ELDH and (E) Au NCs/CoNi-ELDH.

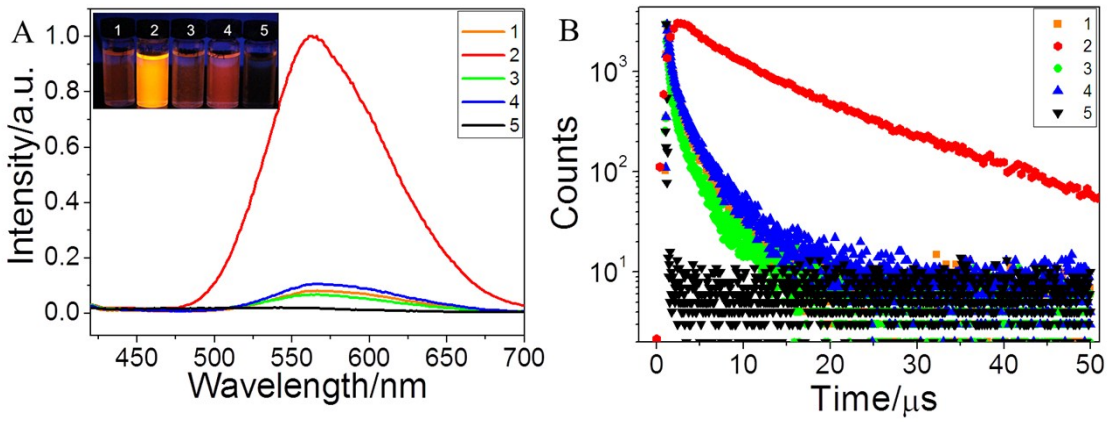

Fig. S11 (A) Fluorescence emission spectra and (B) decay curves of Au NCs-based materials (from 1 to 5: pristine Au NCs, Au NCs/MgAl-ELDH, Au NCs/MMT, Au NCs/PDDA, Au NCs/GO).

Table S6. QYs of Au NCs-based materials with various supports

Sample	Abs.	PL Intensity	QY
Pristine Au NCs	0.0624	7031.5	2.60
Au NCs/MgAl-ELDH	0.0556	46321.5	19.05
Au NCs/MMT	0.0460	5688.6	2.83
Au NCs/PDDA	0.0689	11941.9	3.97
Au NCs/GO	0.0641	1798.7	0.64
Au NCs/CoAl-ELDH	0.0524	11085.6	4.85
Au NCs/CoNi-ELDH	0.0688	14160.6	4.71

Table S7. The fitting of fluorescence decay data of Au NCs-based materials with various supports

Samples	τ_i (μs)	A_i (%)	$<\tau>$ (μs)	χ^2
Pristine Au NCs	0.538	44.10	1.998	1.570
	3.151	55.92		
Au NCs/MgAl-ELDH	6.247	20.61	13.99	1.306
	16.01	79.39		
Au NCs/MMT	0.404	42.33	1.889	1.573
	2.980	57.67		
Au NCs/PDDA	0.571	40.75	2.252	1.535
	3.408	59.25		
Au NCs/GO	0.029	95.36	0.074	1.209
	1.000	4.64		
Au NCs/CoAl-ELDH	0.779	35.32	3.196	1.531
	4.516	64.68		
Au NCs/CoNi-ELDH	0.954	31.64	4.273	1.599
	5.809	68.36		

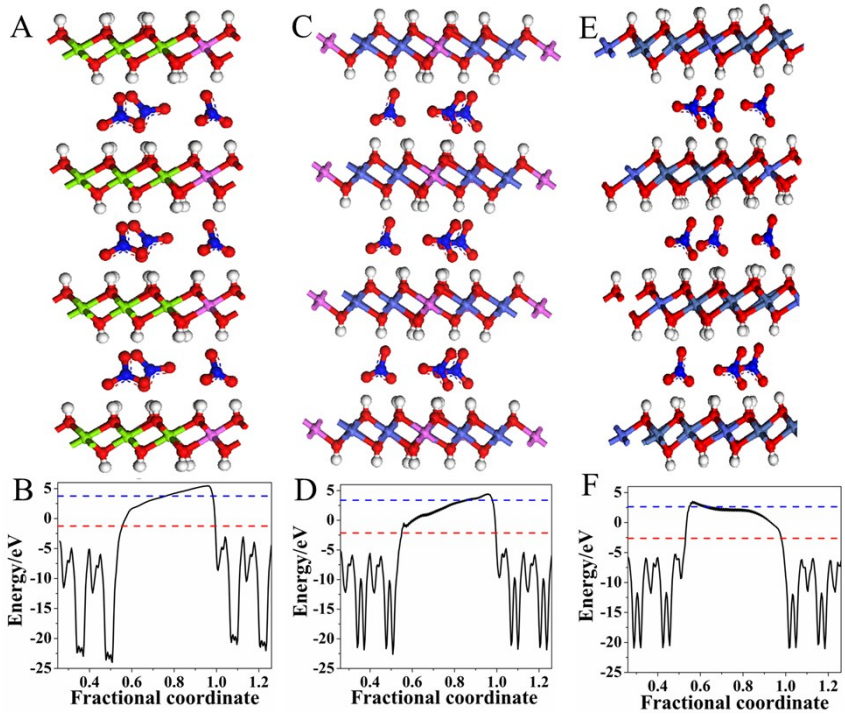

Fig. S12 The optimized geometries and work function of (A, B) MgAl-LDH, (C, D) CoAl-LDH, (E, F) CoNi-LDH, respectively. The red dashed line represents the Fermi level and the blue dashed line denotes the vacuum level; color denotation: red for O, white for H, dark blue for N, green for Mg, pink for Al, blue for Co, and cyan for Ni.

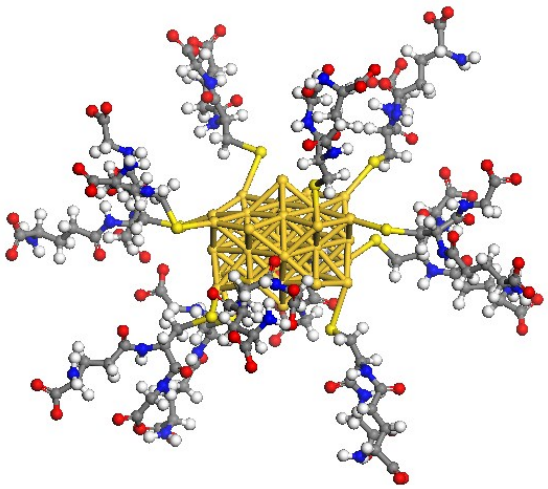

Fig. S13 The optimized geometry of Au NCs (color denotation: red for O, golden for Au, white for H, grey for C, dark blue for N, and yellow for S).

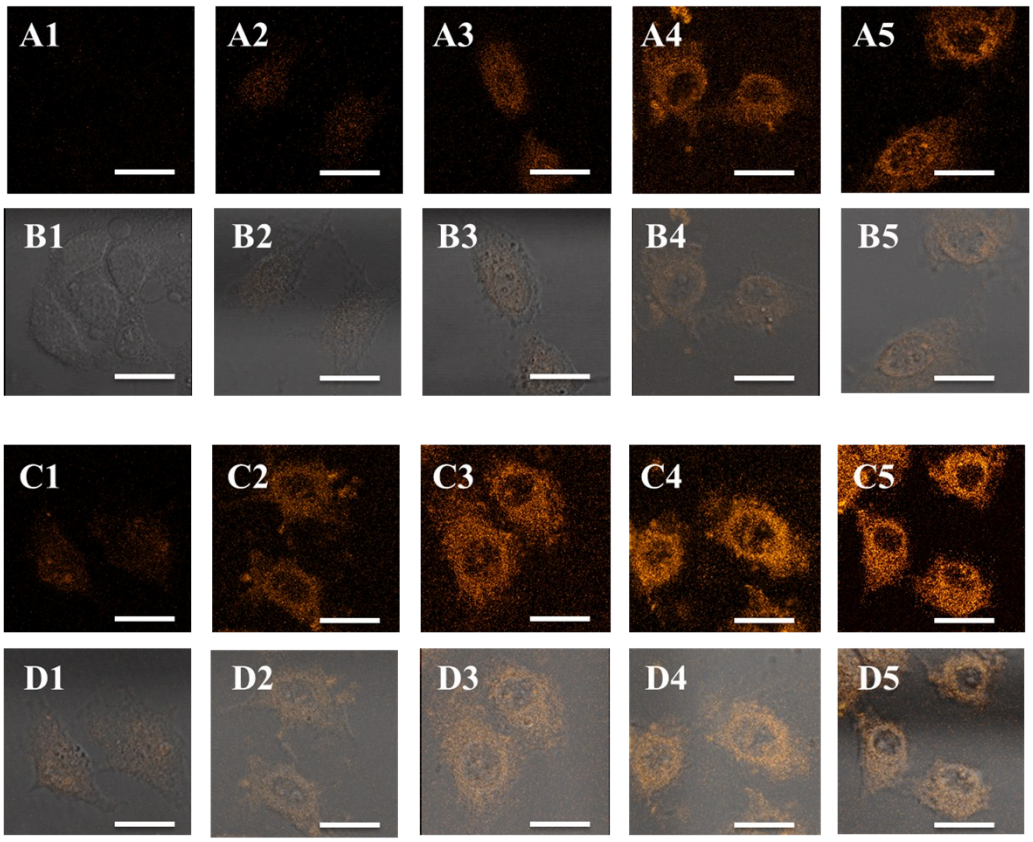

Fig. S14 Fluorescence images of the HeLa cells incubated with (A, B) Au NCs and (C, D) Au NCs/ELDH hybrid material for 24 h (from 1 to 5: the concentration of equivalent Au increases from 6.25 to 12.5, 25, 50 and 100 μg/mL; the scale bar is 10 μm).

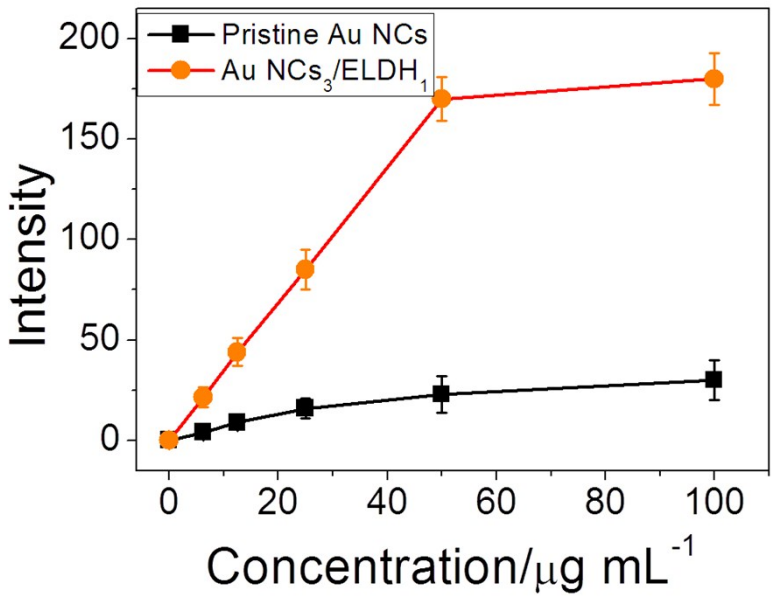

Fig. S15 Fluorescence intensity comparison of Hela cells incubated with Au NCs and Au NCs/ELDH hybrid material with various concentrations.

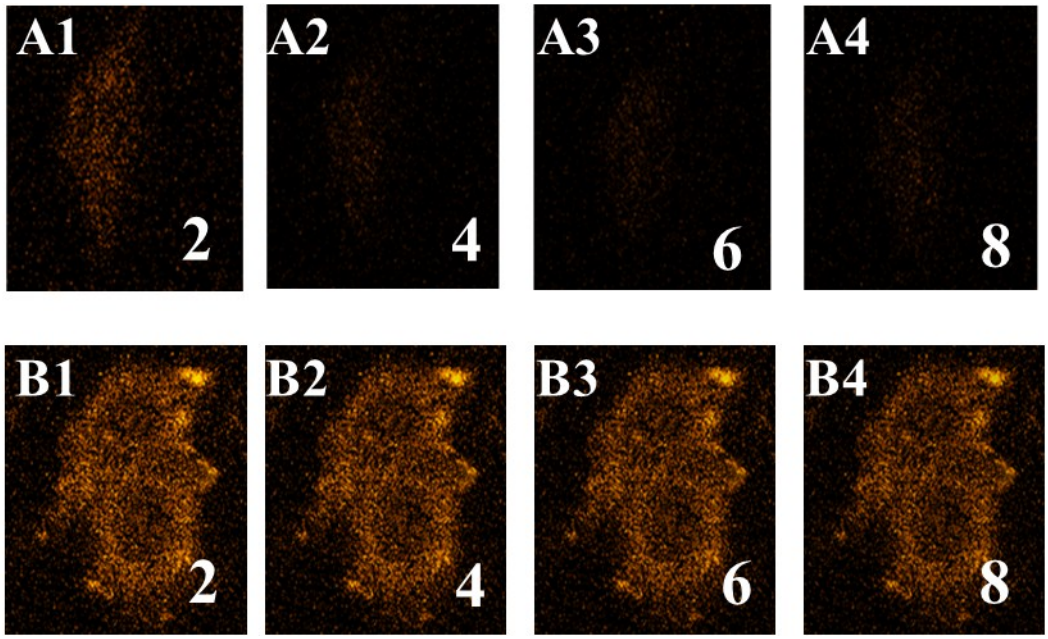

Fig. S16 Stability of (A) Au NCs and (B) Au NCs/ELDH in the cytoplasm of Hela cell captured with an interval of 2 min; the inset shows the sample photographs at 2, 4, 6, 8 min, respectively.

Reference:

1 (*a*) Y.-S. Chen, H. Choi, P. V. Kamat, *J. Am. Chem. Soc.*, 2013, **135**, 8822-8825; (*b*) Z. Luo, X. Yuan, Y. Yu, Q. Zhang, D. T. Leong, J. Y. Lee, J. Xie, *J. Am. Chem. Soc.*, 2012, **134**, 16662-16670; (*c*) C. Wang, Y. Yao, Q. Song, *J. Mater. Chem. C*, 2015, **3**, 5910-5917; (*d*) J. Zhang, Y. Yuan, G. Liang, M. N. Arshad, H. A. Albar, T. R. Sobahi, S.-H. Yu, *Chem. Commun.*, 2015, **51**, 10539-10542.

2 (*a*) R. Liang, D. Yan, R. Tian, X. Yu, W. Shi, C. Li, M. Wei, D. G. Evans, X. Duan, *Chem. Mater.*, 2014, **26**, 2595-2600; (*b*) D. Yan, J. Lu, J. Ma, S. Qin, M. Wei, D. G. Evans, X. Duan, *Angew. Chem. Int. Ed.*, 2011, **50**, 7037-7040.

3 R. Tian, S. Zhang, M. Li, Y. Zhou, B. Lu, D. Yan, M. Wei, D. G. Evans, X. Duan, *Adv. Funct. Mater.*, 2015, **25**, 5006-5015.

4 M. D. Segall, P. J. D. Lindan, M. J. Probert, C. J. Pickard, P. J. Hasnip, S. J. Clark, M. C. Payne, *J. Phys. Condens. Mat.*, 2002, **14**, 2717-2744.

5 S. Xu, T. Pan, Y. Dou, H. Yan, S. Zhang, F. Ning, W. Shi, M. Wei, *J. Phys. Chem. C*, 2015, **119**, 18823-18834.

6 M. Bajdich, M. Garcia-Mota, A. Vojvodic, J. K. Norskov, A. T. Bell, *J. Am. Chem. Soc.*, 2013, **135**, 13521-13530.

7 P.-L. Liao, J. A. Keith, E. A. Carter, *J. Am. Chem. Soc.*, 2012, **134**, 13296-13309.

8 H. C. Andersen, *J. Chem. Phys.*, 1980, **72**, 2384-2393.

9 H. J. C. Berendsen, J. P. M. Postma, W. F. van Gunsteren, A. DiNola, J. R. Haak, *J. Chem. Phys*., 1984, **81**, 3684-3690.

10 M. P. Allen, D. J. Tildesley in *Computer Simulation of Liquids*, Clarendon, Oxford, 1987.

11 T. V. Duncan, M. A. Méndez Polanco, Y. Kim, S.-J. Park, *J. Phys. Chem. C*, 2009, **113**, 7561-7566.